Development 138, 4267-4277 (2011) doi:10.1242/dev.067900

Cell cycle-regulated multi-site phosphorylation of Neurogenin 2 coordinates cell cycling with differentiation during neurogenesis

Fahad Ali[1,*], Chris Hindley[1,*], Gary McDowell[1], Richard Deibler[2], Alison Jones[1], Marc Kirschner[2], Francois Guillemot[3] and Anna Philpott[1,†]

SUMMARY

During development of the central nervous system, the transition from progenitor maintenance to differentiation is directly triggered by a lengthening of the cell cycle that occurs as development progresses. However, the mechanistic basis of this regulation is unknown. The proneural transcription factor Neurogenin 2 (Ngn2) acts as a master regulator of neuronal differentiation. Here, we demonstrate that Ngn2 is phosphorylated on multiple serine-proline sites in response to rising cyclin-dependent kinase (cdk) levels. This multi-site phosphorylation results in quantitative inhibition of the ability of Ngn2 to induce neurogenesis in vivo and in vitro. Mechanistically, multi-site phosphorylation inhibits binding of Ngn2 to E box DNA, and inhibition of DNA binding depends on the number of phosphorylation sites available, quantitatively controlling promoter occupancy in a rheostat-like manner. Neuronal differentiation driven by a mutant of Ngn2 that cannot be phosphorylated by cdks is no longer inhibited by elevated cdk kinase levels. Additionally, phosphomutant Ngn2-driven neuronal differentiation shows a reduced requirement for the presence of cdk inhibitors. From these results, we propose a model whereby multi-site cdk-dependent phosphorylation of Ngn2 interprets cdk levels to control neuronal differentiation in response to cell cycle lengthening during development.

KEY WORDS: Cell cycle, Neuronal differentiation, Ngn2, Phosphorylation, *Xenopus*

INTRODUCTION

During development of the central nervous system, cell cycle lengthening accompanies the transition from stem cell-like to neurogenic divisions, and this is subsequently followed by differentiation (Lange and Calegari, 2010; Miyata et al., 2010). However, recent experiments show that lengthening (but not necessarily arresting) the cell cycle alone by perturbation of the core cell cycle machinery is sufficient to trigger neuronal differentiation, whereas shortening the cell cycle inhibits neurogenesis (Lange et al., 2009). These findings indicate that cell cycle length is itself a regulator of the balance between progenitor maintenance and differentiation, although the mechanism for this regulation is unknown.

The proneural basic helix-loop-helix (bHLH) transcription factor Neurogenin 2 (Ngn2, or Neurog2) is required for development of cranial and spinal sensory ganglia, as well as for the ventral spinal cord (Bertrand et al., 2002). Moreover, in the embryonic cortex, Ngn2 is required for neuronal commitment and inhibition of the astrocytic fate of progenitors, as well as for the specification of glutamatergic neurotransmitter identity and the migration of cortical neurons (Bertrand et al., 2002). Ngn2 has been shown to transcriptionally upregulate multiple direct targets. Among these, one crucial Ngn2 target is the bHLH transcription factor NeuroD, which plays a central role in driving neuronal differentiation.

Although transcriptional regulation of *Ngn2* itself is complex, evidence has emerged of additional Ngn2 control by post-translational modification. A limited exploration of the role of phosphorylation in Ngn2 activity has been undertaken (Hand et al., 2005; Vosper et al., 2007; Ma et al., 2008). For example, phosphorylation of tyrosine 241 in Ngn2 is important for the migration and dendritic morphology of cortical neurons (Hand et al., 2005) and phosphorylation on two specific C-terminal serines, which are GSK3β consensus sites, appears to have no effect on neurogenesis per se in the spinal cord but does regulate motoneuron specification in this tissue (Ma et al., 2008).

Ngn2 protein level is regulated by ubiquitin-mediated proteolysis, and the rate of proteolysis is sensitive to cell cycle stage; *Xenopus* Ngn2 [xNgn2, also known as XNgnR1 (Nieber et al., 2009)], the frog homologue of mammalian Ngn2 (Ma et al., 1996; Nieber et al., 2009), has a shorter half-life in mitosis than in interphase (Vosper et al., 2009). Accumulation of cyclin-dependent kinase inhibitors (cdkis), which occurs upon cell cycle lengthening and exit, promotes neurogenesis mediated by Ngn2 (Vernon et al., 2003). Surprisingly, this particular effect of cdkis is independent of their ability to inhibit cdk kinase activity, but instead results from an independent role for cdkis in stabilising the Ngn2 protein (Vernon et al., 2003; Nguyen et al., 2006). In addition, it is also possible that Ngn2 protein undergoes other post-translational modifications, including phosphorylation, that might be used to coordinate its activity with cell cycle progression.

Cyclin A/*cdk2* overexpression inhibits primary neurogenesis in *Xenopus* embryos. Moreover, ectopic neurogenesis in embryos driven by *Ngn2* mRNA injection is still inhibited by cdk activation

[1]Department of Oncology, University of Cambridge, Hutchison/Medical Research Council (MRC) Research Centre, Cambridge CB2 0XZ, UK. [2]Department of Systems Biology, Harvard Medical School, 200 Longwood Avenue, Boston, MA 02115, USA. [3]Division of Molecular Neurobiology, National Institute for Medical Research, Mill Hill, London NW7 1AA, UK.

*These authors contributed equally to this work
†Author for correspondence (ap113@cam.ac.uk)

Accepted 18 July 2011

(Richard-Parpaillon et al., 2004), indicating that cell cycle control does not occur at the level of *Ngn2* transcription. Instead, cell cycle-dependent post-translational regulation of Ngn2 protein has the potential to directly regulate the ability of Ngn2 to drive neuronal differentiation. Here, we demonstrate how multi-site post-translational modification of Ngn2 is used as a sensor of cdk kinase levels to balance progenitor maintenance and differentiation, in coordination with cell cycle length.

MATERIALS AND METHODS

Xenopus laevis extracts and embryos

Acquisition of *Xenopus laevis* eggs and embryos, preparation and injection of synthetic mRNA and DNA morpholinos, staging of embryos, in situ hybridisation and egg extract preparation have been described previously (Vernon et al., 2003; Vosper et al., 2007; Vosper et al., 2009).

In vitro translated (IVT) protein synthesis and assay

Degradation assays were performed as described previously (Vosper et al., 2007; Vosper et al., 2009). Phosphorylation assays in *Xenopus* extract were performed as for degradation assays, except that extract was supplemented with 0.2 mM MG132 (Biomol) and samples were incubated for 45 minutes unless otherwise indicated. Where indicated, extracts were supplemented with the GSK3 inhibitor (2′Z,3′E)-6-bromoindirubin-3′-oxime (BIO) (Sigma) at 100 nM or with roscovitine (VWR) at 50 mM. Where indicated, following the 45 minute incubation in extract, 400 units λ-phosphatase (NEB) were incubated with the sample at 30°C for 30 minutes.

Cell culture, transfection, immunocytochemistry and western blotting

Mouse P19 cells were cultured in α-MEM (Gibco) with 7.5% newborn calf serum and 2.5% fetal bovine serum (HyClone), 1% Glutamax (Gibco), and 100 units/ml penicillin/100 μg/ml streptomycin (Sigma). Cells were transfected with Lipofectamine 2000 (Invitrogen), and extracts western blotted with anti-HA-peroxidase (3F10; Roche) or anti-c-Myc (9E10; Santa-Cruz). Where indicated, cells were treated with either 5-25 μm roscovitine or 400 units λ-phosphatase. P19 cells plated on poly-D-lysine and laminin (Sigma) and fixed in 4% formaldehyde for 15 minutes were stained with anti-TuJ1 (neuronal class III β-Tubulin; 1:200; Covance) and chicken anti-green fluorescent protein (GFP; 1:500; Invitrogen).

Somatic cell extract preparation for Ngn2 phosphorylation assay

Somatic cell extracts were prepared as described previously (Deibler and Kirschner, 2010).

Quantitative real-time PCR (qPCR)

cDNA was generated from either P19 cells or stage 15 *Xenopus* embryos and 50 ng used per qPCR reaction in a Light-Cycler 480 PCR system with SYBR Green mix (Roche). β-actin, *Gapdh* and *EF1α* were used as housekeeping genes. Thermal cycling conditions: 95°C for 5 minutes, then 45 cycles of 95°C for 10 seconds, 60°C for 10 seconds and 72°C for 10 seconds. For primer sequences, see Table S1 in the supplementary material.

Electrophoretic mobility shift assay (EMSA)

Non-radiolabelled IVT protein was prepared and incubated in XB buffer or *Xenopus* egg extract as for phosphorylation assays before EMSA analysis as previously described (Vosper et al., 2009), using the annealed, end-labelled oligonucleotide pair (5′-TCTAACTGGCGACAGATGGG-CCACTTTCTT-3′ and complement).

Chromatin Immunoprecipitation assay (ChIP)

DNA-protein complexes from P19 cells transfected with either HA-tagged wild-type mNgn2 or 9S-A mNgn2 for 24 hours and normalised for mNgn2/9S-A mNgn2 expression (see Results) were cross-linked with 1% formaldehyde. Five micrograms of rat monoclonal anti-HA antibody (Roche) or anti-IgG (Abcam) (as a control) were used per ChIP reaction and quantified using SYBR Green mix. The signal over background normalisation method was used to quantify immunoprecipitated DNA. For primer sequences, see Table S1 in the supplementary material.

Statistical analysis

Data were subjected to statistical analysis using a two-tailed Student's *t*-test ($P \leq 0.05$). The standard error of the mean (s.e.m.) was calculated from at least three independent experiments. Immunostaining, western blotting and in situ hybridisation experiments were performed in three independent experiments and representative results are shown.

RESULTS

Neurogenin 2 phosphorylation is regulated during the cell cycle

Ngn2 phosphorylation has previously been demonstrated on tyrosine and GSK3β consensus sites (Hand et al., 2005; Vosper et al., 2007; Ma et al., 2008), but cell cycle-dependent phosphorylation has not been investigated. We have previously observed that Ngn2 protein can be phosphorylated in *Xenopus* egg extract, which provides a complex biochemical environment that contains stockpiles of many of the kinases and phosphatases required for cell cycle transitions and early embryonic

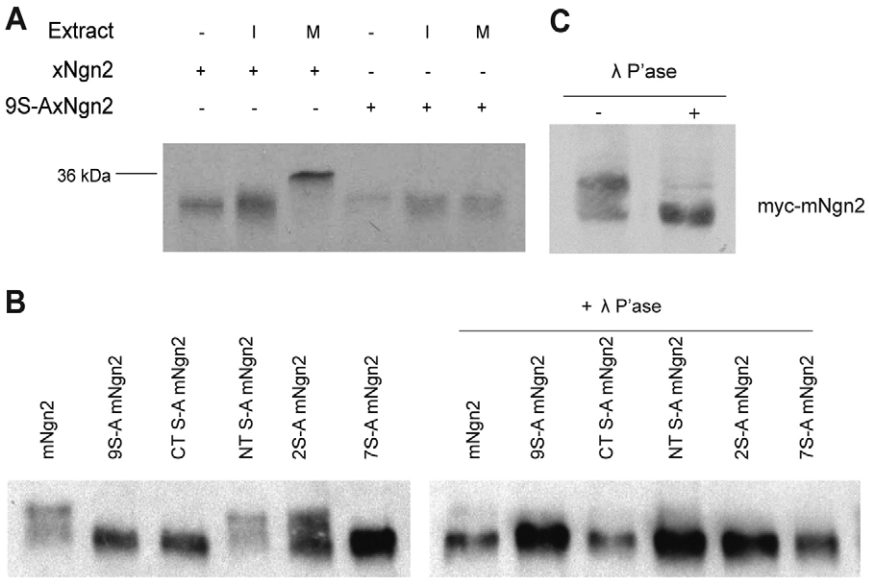

Fig. 1. Ngn2 undergoes cell cycle-regulated phosphorylation. (**A**) In vitro translated (IVT) [^{35}S]methionine-labelled xNgn2 and 9S-A xNgn2 were incubated in interphase (I) and mitotic (M) *Xenopus* egg extracts before SDS-PAGE and autoradiography. In M extracts, phosphorylated xNgn2 runs at the level of the 36 kDa molecular weight marker (indicated). (**B**) Western blot analysis of HA-tagged mNgn2 and mutants thereof, transfected into mouse P19 cells with and without λ-phosphatase treatment. (**C**) Western blot analysis of myc-mNgn2 from E16.5 mouse cortex, with and without λ-phosphatase treatment.

development, and results in slowed migration of Ngn2 in SDS-PAGE (Vosper et al., 2007). We hypothesised that this phosphorylation might be regulated by the cell cycle.

We compared SDS-PAGE migration of in vitro translated (IVT) [^{35}S]methionine-labelled *Xenopus* Ngn2 (xNgn2) in interphase egg extract (I) or in extract driven into mitosis (M) by addition of non-degradable cyclin B Δ90 (King et al., 1996). IVT xNgn2 runs at ~28 kDa by SDS-PAGE, and its migration is slowed slightly after incubation in I extract (Fig. 1A), and more dramatically after incubation in M extract, resulting in the appearance of one or more forms of Ngn2 running up to 8 kDa 'larger' (Fig. 1A, see Fig. S2 in the supplementary material). Retardation was reversed by incubation with λ-phosphatase (data not shown).

Although predictions of consensus sequences that contribute to kinase recognition are imprecise (Errico et al., 2010), several prominent kinases potentially present in the egg extract, such as cdks, MAP kinases and GSK3β, preferentially phosphorylate on serine or threonine residues followed by a proline (SP or TP sites) (Ubersax and Ferrell, 2007). xNgn2 contains nine SP and one TP site. To prevent phosphorylation on SP sites, a mutant form of xNgn2, 9S-A xNgn2, in which all SP sites are mutated to alanine-proline (S-A mutant) was generated. 9S-A xNgn2 ran similarly to the IVT protein after incubation in I or M extracts (Fig. 1A), indicating that the phosphorylation seen for the wild-type protein does not occur on 9S-A xNgn2. We did not detect significant phosphorylation of the TP site by SDS-PAGE migration (data not shown), and did not consider modification of this site further.

Mouse Ngn2 (mNgn2) can drive neuronal differentiation of mouse embryonal carcinoma P19 cells when overexpressed (Farah et al., 2000), and also contains nine SP sites. However, only the position of the two most C-terminal GSK3β consensus sites, which have previously been shown to be phosphorylated in spinal cord (Ma et al., 2008), is conserved with xNgn2. After transfection into P19 cells, at least two phosphoforms of mNgn2 were seen, as evidenced by migration in SDS-PAGE and phosphatase treatment, whereas 9S-A mNgn2 ran as a single, faster migrating band (Fig. 1B). Further analysis of Ngn2 mutants in which SP sites in the N- and C-termini have been separately mutated shows that xNgn2 and mNgn2 are both phosphorylated on multiple sites in both the N- and C-terminal domains (Fig. 1B, see Fig. S2 in the supplementary material). Analysis of phosphorylation of 2S-A Ngn2 (which lacks the potential GSK3β sites) and 7S-A Ngn2 (in which only the two potential GSK3β SP sites are present in an otherwise S-A background) indicates that phosphorylation does not predominantly occur on these GSK3β SP sites (Fig. 1B).

To determine the phosphorylation status of Ngn2 expressed from its endogenous locus, we investigated the migration of a myc-tagged form of mNgn2 in embryonic brain from a mouse line in which *myc-mNgn2* is inserted in the place of endogenous *mNgn2* (Hand et al., 2005). Western blotting demonstrated that mNgn2 is phosphorylated in the developing mouse brain (Fig. 1C).

Ngn2 is phosphorylated on multiple sites by cyclin-dependent kinases

Cdks drive cell cycle progression and are known to target SP (and TP) sites (Errico et al., 2010). We postulated that Ngn2 might be a direct cdk substrate. Addition of roscovitine, a chemical cdk inhibitor with marked specificity for cdks alone (Bain et al., 2007), results in a dose-dependent reduction of the slower migrating form of mNgn2 expressed in P19 cells (Fig. 2A). Roscovitine also reversed the reduction in mobility seen when xNgn2 was incubated in neurula stage *Xenopus* embryo extracts (see Fig. S3 in the supplementary material).

To quantitatively analyse the sensitivity of Ngn2 to increasing cdk activity, we turned to an in vitro human HeLa cell extract system that exhibits quantitative cyclin dose-dependent effects on substrate phosphorylation (Deibler and Kirschner, 2010), as evidenced by slowed migration in SDS-PAGE, and recapitulates cell cycle-relevant transitions. From entry into S phase through prometaphase, cyclin A concentration increases in the cell, and this can be reproduced by increasing the dose of cyclin in the cell extract (Deibler and Kirschner, 2010). mNgn2 is highly sensitive to cyclin A-dependent kinase, and phosphorylation is evident when only 12.5 nM cyclin A is added (Fig. 2B). As the cyclin A

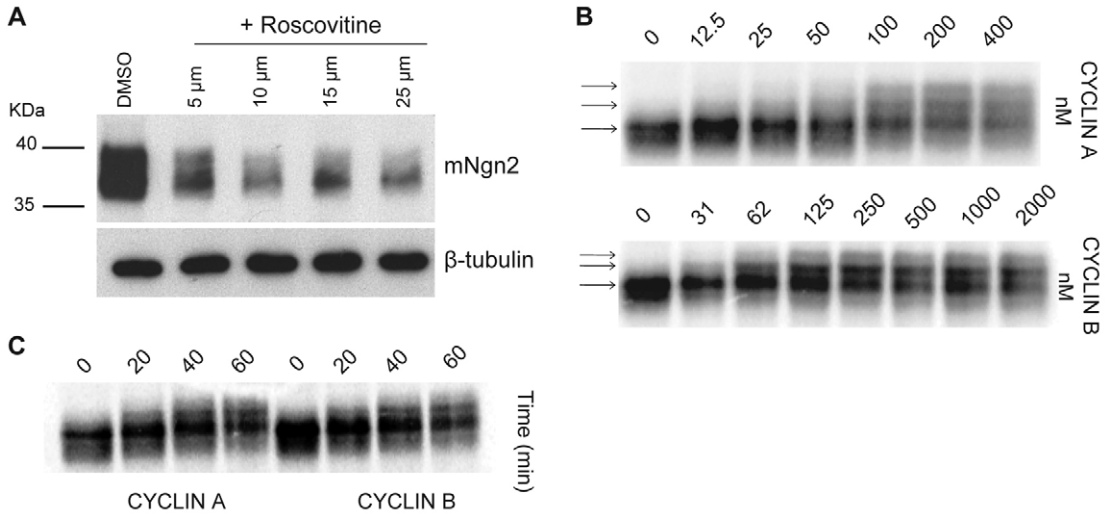

Fig. 2. Ngn2 is phosphorylated by cyclin-dependent kinases. (**A**) Western blot analysis of HA-tagged mNgn2 and 9S-A mNgn2 24 hours after transfection into mouse P19 cells with and without treatment with the cdk inhibitor roscovitine. β-Tubulin provides a loading control. (**B**) SDS-PAGE analysis of IVT mNgn2 in human HeLa cell extract in response to increasing doses of recombinant cyclin A (top) or cyclin B (bottom). Arrows indicate different phosphoforms of mNgn2. (**C**) SDS-PAGE analysis of the kinetics of phosphorylation of IVT mNgn2 when added to HeLa extracts containing recombinant cyclin A or cyclin B proteins.

concentration rises, at least two or three increasingly retarded mNgn2 forms appear (Fig. 2B), indicating that mNgn2 is phosphorylated on multiple sites. That slower migrating phosphoforms require higher cyclin A concentrations demonstrates that there is no single threshold at which multiple sites are phosphorylated, but rather that the extent of phosphorylation is sensitive to the level of kinase activity. Above 100 nM cyclin A, when cyclin A-dependent kinase levels are saturating, the fastest migrating mNgn2 band is lost, indicating that all Ngn2 is essentially phosphorylated. These results demonstrate that mNgn2, together with Wee1, is one of the most sensitive substrates of cyclin A-dependent kinase currently known (Deibler and Kirschner, 2010), although in contrast to Wee1, as cyclin A levels rise mNgn2 becomes further phosphorylated on additional sites.

The addition of cyclin B to these G2 phase HeLa extracts leads to triphasic cdk kinase activation: a first phase in which cdk kinase activity increases in proportion to cyclin B up to ~100 nM, followed by a plateau of kinase activity between 125-400 nM, and finally a further increase to saturation above 400 nM (Deibler and Kirschner, 2010). mNgn2 is also highly sensitive to cyclin B-dependent kinase (Fig. 2B), showing phosphorylation at the lowest concentration of cyclin B assayed, 31 nM, with maximal phosphorylation at additional sites achieved around the plateau stage from 125 nM cyclin B upwards, indicating dose-dependent sensitivity to cdk kinase levels.

Ngn2 phosphorylation is rapid. After addition of cyclins A or B, histone H1 kinase levels become maximal after a 16-minute lag required for cdk kinase activation. When mNgn2 was added to these extracts, initial phosphorylation at some sites occurred within 20 minutes (Fig. 2C), but additional phosphorylations took longer, indicating that some sites are phosphorylated before others and that phosphorylation continues over a considerable period. We see greater phosphorylation in these mitosis-like extracts than in P19 lysates from asynchronous P19 cells representing all cell cycle stages, where interphase will predominate (Fig. 1). Immunodepletion of specific cdks from HeLa extracts indicates that Ngn2 is a substrate of both cdk1 and cdk2 (see Fig. S4 in the supplementary material).

Phosphorylation of Ngn2 reduces its ability to induce neuronal differentiation

Ngn2 can be phosphorylated on multiple sites by cdks. What is the effect of phosphorylation on Ngn2 activity in the developing embryo? To distinguish effects of post-translational modification from fluctuating levels of *Ngn2* transcripts, which vary from cell to cell and as development progresses (Ma et al., 1996; Bertrand et al., 2002; Shimojo et al., 2008), we chose to express xNgn2 from microinjected mRNA in order to allow us to control the level of xNgn2 expression in vivo in *Xenopus* embryos that are at the correct developmental stage to provide the physiological response of primary neuron differentiation (Ma et al., 1996).

Injection of 5 pg *xNgn2* mRNA results in a small increase in neurogenesis within the neural plate in individual embryos, but little ectopic neurogenesis outside the neural plate, indicating a similar level of expression to endogenous *xNgn2* mRNA. Injection of 5 pg *9S-A xNgn2* mRNA, by contrast, induces both a significant increase in neurogenesis in the neural plate and is sufficient to change the fate of epidermis to differentiated neurons (Fig. 3A) (Ma et al., 1996). At 20 pg mRNA, *xNgn2* was still only able to induce a modest increase in neurogenesis, although now neurons were present outside the neural plate, whereas the same amount of *9S-A xNgn2* mRNA induced very extensive neurogenesis (Fig. 3A). Quantitation of *neural* β*-tubulin* levels in these neural plate stage embryos by qPCR demonstrates that *9S-A xNgn2* is ~7-fold more active than wild-type *xNgn2* when expressed at near physiological levels in *Xenopus* embryos (Fig. 3B).

Testing of seven mutants, in which individual SP sites had been reintroduced into a phosphomutant xNgn2 background, demonstrated a similar level of activity of each to 9S-A xNgn2 (see Fig. S5 in the supplementary material), indicating that no individual SP site is responsible for substantially limiting Ngn2 activity, but instead that phosphorylation at a combination of sites might be required to limit the ability of Ngn2 to induce neurogenesis.

Mutation of SP sites also promotes Ngn2-driven neurogenesis in P19 cells. Significantly more extensive neurogenesis was seen in P19 cells expressing 9S-A mNgn2 than in cells expressing wild-type mNgn2, as measured by TuJ1 staining (Fig. 3C) and confirmed by qPCR analysis (Fig. 3D). Analysis of mutants indicated that potential phosphorylation on the GSK3β sites might contribute to phosphoregulation of Ngn2 activity to a small extent, but that phosphorylation of other sites accounts for the majority of the inhibition of Ngn2-dependent neuronal differentiation (see Fig. S6 in the supplementary material).

Mechanism of regulation of Ngn2 activity by phosphorylation

The transcriptional activation of promoters of genes promoting differentiation may require many cycles of productive transcription factor binding and greater promoter occupancy to bring about progressive chromatin modification, ultimately resulting in an active transcribable state (Koyano-Nakagawa et al., 1999; Hager et al., 2009; Michel, 2009). Ngn2 must bind and activate the promoters of key target genes, such as *NeuroD*, to drive neuronal differentiation. Hence, we reasoned that phosphorylation might affect Ngn2 half-life or its ability to stably bind to promoter DNA, either of which could affect the duration and/or productivity of the interaction between Ngn2 and target promoters driving differentiation.

We first investigated whether phosphorylation status affects Ngn2 protein stability. Ngn2 has a short half-life of ~20 minutes in *Xenopus* and P19 cells, which is enhanced by binding to its heterodimeric E protein partner (Vosper et al., 2007). We determined whether phosphorylation directly affects Ngn2 half-life by incubating IVT xNgn2 or 9S-A xNgn2 in I and M extract. The half-life of 9S-A xNgn2 was similar to that of xNgn2 in both I and M (Fig. 4A) and in neurula stage *Xenopus* embryo extracts (data not shown). Addition of E12 protein stabilised xNgn2 and 9S-A xNgn2 in both I and M extracts (Fig. 4A). However, in M extract, where cdk-dependent phosphorylation is maximal, E12 stabilised 9S-A xNgn2 to a greater extent than it stabilised the wild-type protein. Hence, the phosphorylation status of Ngn2 affects its ability to be stabilised by E protein binding; un(der)phosphorylated, and therefore more stable, Ngn2-E protein complexes might be expected to show greater promoter occupancy than the phosphorylated form of the protein.

To test this we investigated whether phosphorylation affects Ngn2 binding to the *NeuroD* (*Neurod1*) and *Delta* (*Dll1*) promoters, which are direct downstream targets of Ngn2, by chromatin immunoprecipitation (ChIP) in P19 cells, 24 hours post-transfection. As described above, phosphorylation status affects the stabilisation of Ngn2 by E proteins (Fig. 4A). To distinguish differences in chromatin affinity from potential differences in mNgn2 and 9S-A mNgn2 protein levels, we quantitated the

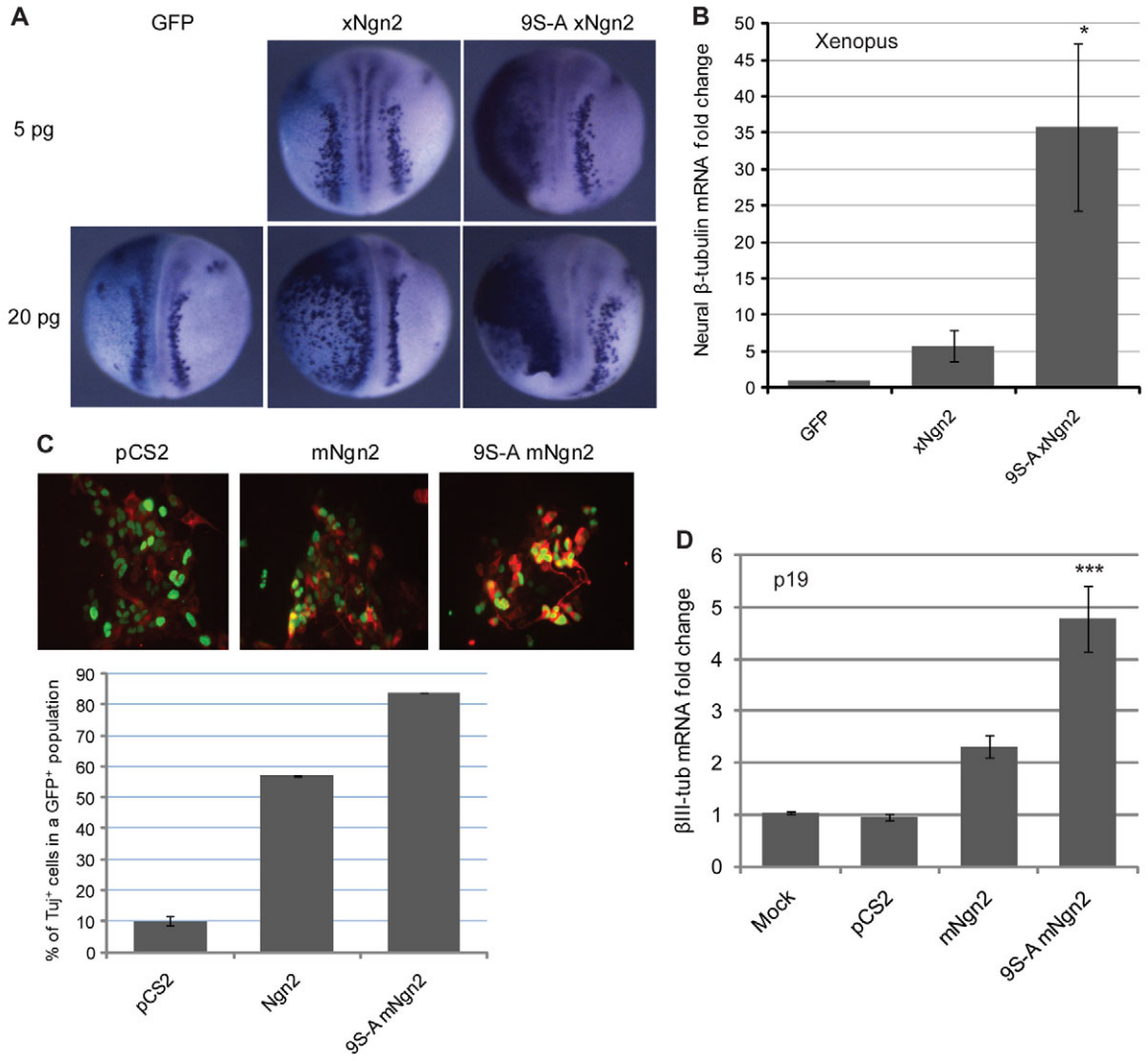

Fig. 3. Mutation of phosphorylation sites promotes Ngn2 activity. (**A**) *Xenopus* embryos were injected (left side) in one of two cells with either 5 or 20 pg mRNA as indicated, fixed at stage 15 and subject to in situ hybridisation for *neural* β-*tubulin*. The number of embryos scored was 39-90 per condition. (**B**) qPCR analysis of *neural* β-*tubulin* in stage 15 *Xenopus* embryos injected at the one-cell stage with 20 pg *xNgn2* or *9S-A xNgn2* mRNA. Average fold increase in *neural* β-*tubulin* mRNA expression is shown normalised to *GFP*-injected control (mean ± s.e.m.; *, $P \leq 0.05$). (**C**) Mouse P19 cells transfected with *mNgn2* or *9S-A mNgn2* with GFP were fixed 24 hours after transfection and stained for expression of neuron-specific *βIII-tubulin* (TuJ1) (red), quantitating TuJ1$^+$ among GFP$^+$ cells (mean ± s.e.m.). (**D**) qPCR analysis of *βIII-tubulin* in P19 cells 24 hours following transfection with *mNgn2* and *9S-A mNgn2*. Average fold increase in mRNA expression is shown normalised to housekeeping gene expression (mean ± s.e.m.; ***, $P \leq 0.005$).

expression of wild-type mNgn2 versus 9S-A mNgn2 by western blot, allowing normalisation of the amount of Ngn2 protein prior to chromatin immunoprecipitation. After normalisation, 9S-A mNgn2 was more than 2-fold enriched compared with wild-type mNgn2 on each promoter, but promoter-specific differences in mNgn2 versus 9S-A mNgn2 binding were not observed (Fig. 4B).

To test directly whether phosphorylation of Ngn2 affects its ability to associate with DNA, we investigated the binding of xNgn2-E12 complexes to their cognate E box-binding motif in an electrophoretic mobility shift assay (EMSA) in I and M extracts. Wild-type xNgn2 and 9S-A xNgn2 had similar DNA-binding activity in I extract, where xNgn2 phosphorylation is low, but 9S-A xNgn2-E12 bound DNA with considerably greater affinity than the wild-type protein in M extracts, where Ngn2 phosphorylation is maximal (Fig. 4C).

Multi-site phosphorylation of Ngn2 acts quantitatively to control DNA binding

Promoter activation requires productive transcription factor binding cycles, which in turn depend on the strength and/or duration of promoter occupancy by that transcription factor. Phosphorylation of Ngn2 occurs on multiple sites, which together can regulate DNA and promoter binding. We investigated whether specific SP sites are responsible for Ngn2 phosphoregulation or whether regulation is attained by the additive effect of individual phosphorylation events, each one quantitatively having a small effect on promoter occupancy by Ngn2, the number of sites phosphorylated being quantitatively dependent on the cdk kinase level (Fig. 2). We tested whether the mutation of an increasing number of phosphorylation sites had an additive effect on Ngn2 DNA binding and its ability to induce neuronal differentiation.

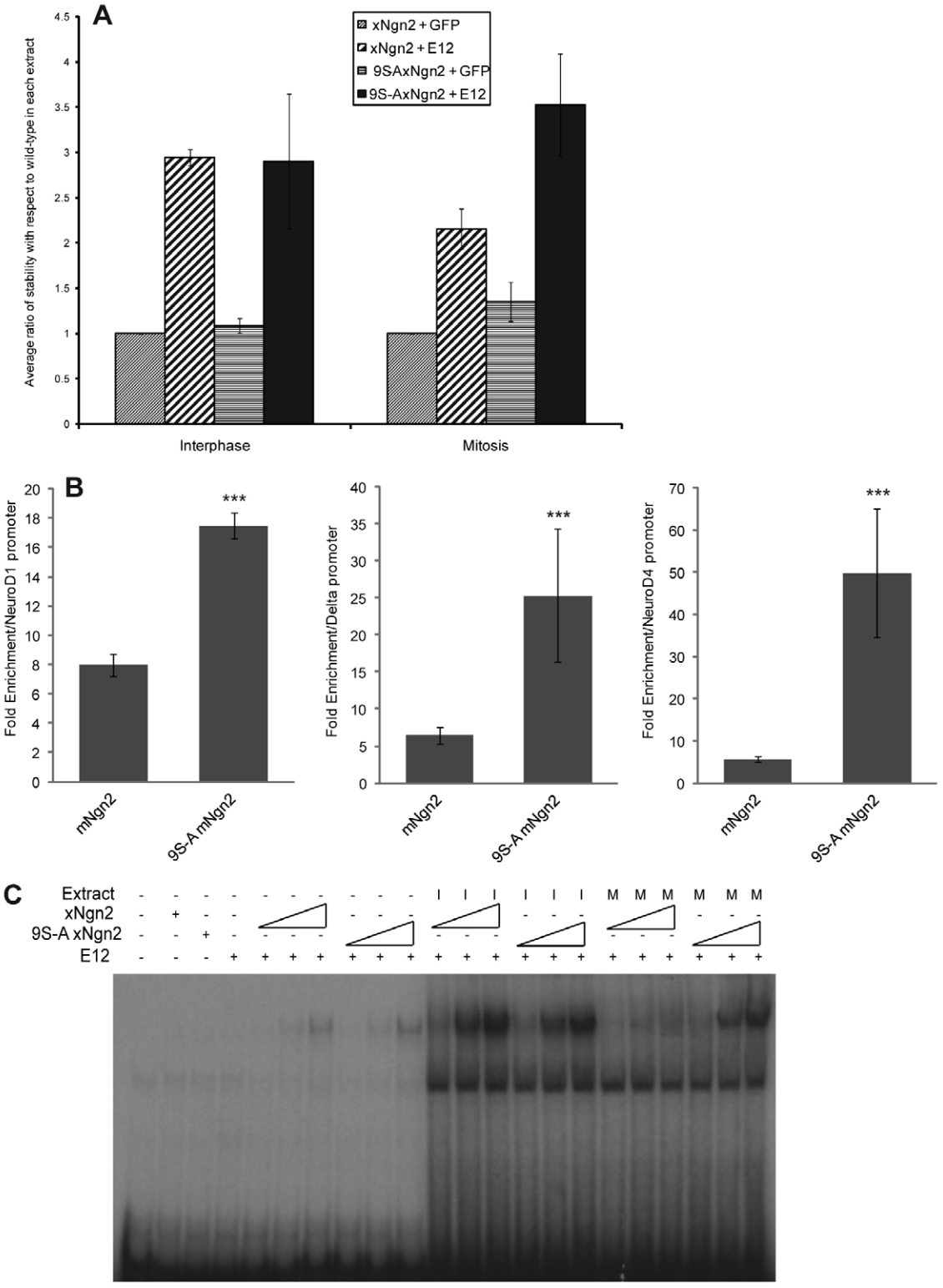

Fig. 4. Phosphomutant Ngn2 binds more efficiently than wild-type Ngn2 protein to DNA and is stabilised more by E12. (**A**) IVT [^{35}S]methionine-labelled xNgn2 or 9S-A xNgn2 were incubated in I or M *Xenopus* egg extracts in the presence of unlabelled IVT GFP or E12. Samples were removed every 10 minutes, separated by SDS-PAGE and the amount of Ngn2 protein determined by phosphorimaging, calculating the half-life of Ngn2 protein degradation using first-order rate kinetics. Half-lives were normalised to that of xNgn2 with GFP in each experiment and the average ratios of stability relative to xNgn2 with GFP for three experiments were plotted (mean ± s.e.m.). (**B**) Chromatin immunoprecipitation (ChIP) analysis of cell extracts containing normalised amounts of HA-tagged mNgn2 and 9S-A mNgn2, assessing binding to the promoters of *Neurod1*, delta-like 1 (*Dll1*) and *Neurod4* in mouse P19 cells, 24 hours following transfection (IgG control for non-specific background binding). ***, $P \leq 0.005$. (**C**) Electrophoretic mobility shift assay (EMSA) showing E box binding of normalised IVT xNgn2 or 9S-A xNgn2 in I and M extracts with and without E12.

A panel of S-A mutant versions of mNgn2 was constructed in which the mutation of SP sites was undertaken additively from the N-terminus (i.e. mS-A1 has the most N-terminal SP site mutated to AP, mS-A2 has the first two N-terminal sites mutated, and so on; see Fig. S1 in the supplementary material), and their DNA binding tested by EMSA. As previously seen with xNgn2 and 9S-A xNgn2 (Fig. 4C), there was little difference in the DNA binding of any of our additive mNgn2 phosphomutants in I extract (see Fig. S7 in the supplementary material). However, in M extract, the E box binding increases progressively as phosphorylation sites are lost (Fig. 5A).

To determine whether the number of SP sites available for phosphorylation is more important than the location of those sites, we investigated a series of xNgn2 phosphomutants in which SP sites were additively mutated, but this time from the C-terminus (see Fig. S1 in the supplementary material). Again, we saw that the availability of SP sites quantitatively regulates DNA binding in M; as each SP site was additionally mutated, DNA-binding activity progressively increased (Fig. 5A). Thus, phosphorylation of multiple SP sites can act quantitatively, in a rheostat-like manner, to control E box binding by mNgn2 and

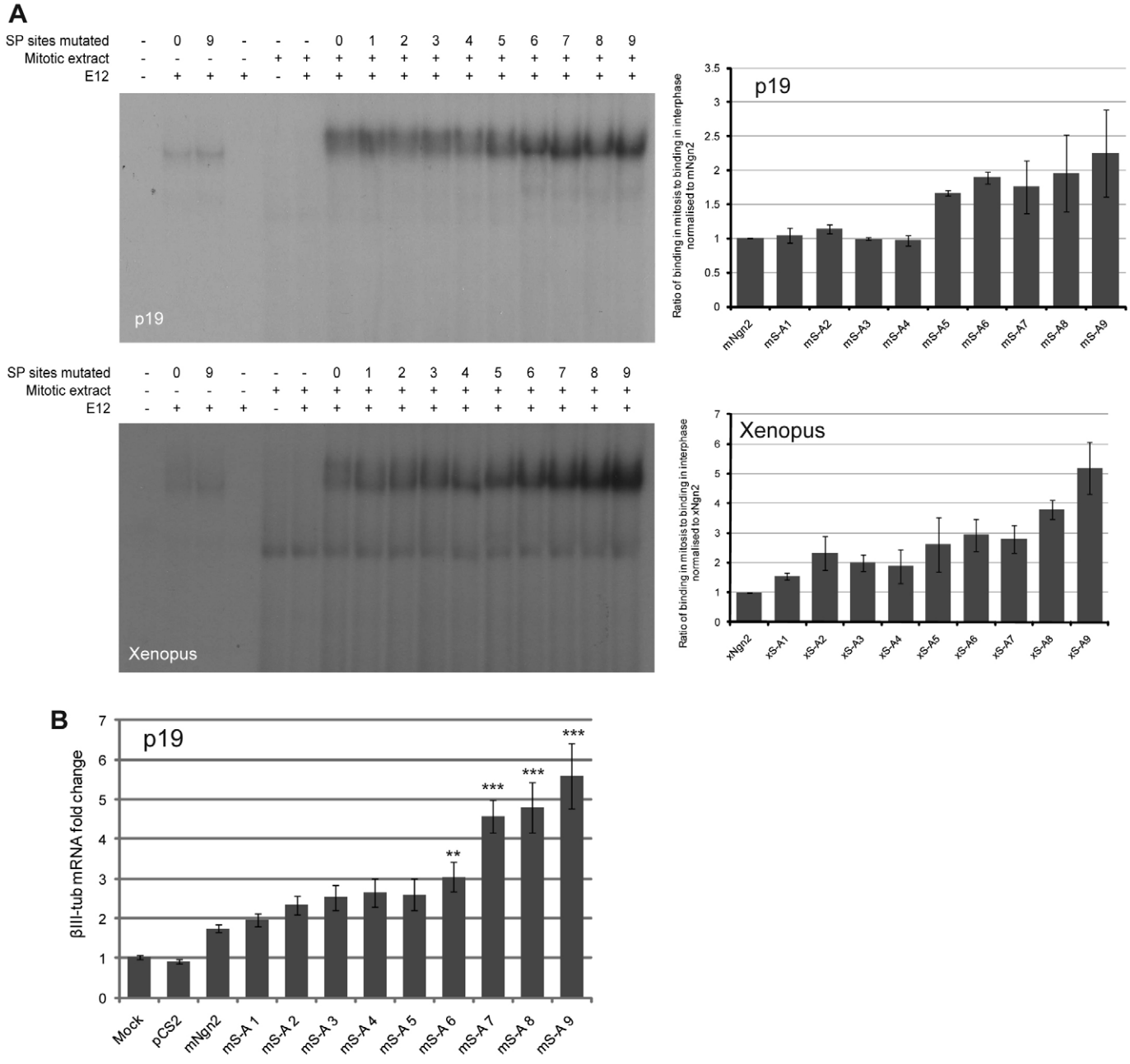

Fig. 5. Phosphorylation on multiple serine-proline (SP) sites has an additive effect on Ngn2 DNA binding. (**A**) EMSA analyses in *Xenopus* M extracts showing E box binding of normalised IVTs of xNgn2 or mNgn2 and additive phosphorylation site mutants of *xNgn2* or *mNgn2* as labelled. Graphs show quantitation of E box binding of phosphorylation site mutants by phosphorimaging, normalised to DNA binding of xNgn2 or mNgn2 as appropriate (see Fig. S1 in the supplementary material). (**B**) qPCR analysis of neural *βIII-tubulin* in P19 cells. P19 cells were transiently transfected with *mNgn2* and additive phosphorylation site mutants thereof for 24 hours. Average fold increase (± s.e.m.) in *βIII-tubulin* mRNA expression normalised to housekeeping genes [β-actin (*Actb*) and *Gapdh*]. **, $P \leq 0.05$; ***, $P \leq 0.005$.

xNgn2, even though the context and location of only the two most C-terminal SP sites are conserved between these two species.

We next investigated whether the ability of Ngn2 to induce neuronal differentiation of P19 cells is quantitatively dependent on the number of phosphorylation sites available. Using our mNgn2 phosphomutant series (see Fig. S1 in the supplementary material), we saw a fairly gradual increase in βIII-tubulin expression as additional SP sites were mutated (Fig. 5B), demonstrating that the propensity of Ngn2 to drive neuronal differentiation depends, at least semi-quantitatively, on the number of phosphorylation sites available. However, mutation of the final three (most C-terminal) SP sites had the biggest effect.

Cell cycle regulators control neuronal differentiation by post-translational regulation of Ngn2 protein

Enhancing cdk activity inhibits neurogenesis in vivo (Richard-Parpaillon et al., 2004; Lange et al., 2009). The results presented above led us to hypothesise that its inhibitory activity is via post-translational modification of the Ngn2 protein, and so phosphomutant Ngn2 would not be susceptible to inhibition by *cyclin A*/*cdk2* overexpression. To test this, we chose to inject levels of *xNgn2* mRNA that induce limited ectopic neurogenesis, largely within the neural plate, to mimic in vivo expression levels.

As previously reported, injection of *cyclin A*/*cdk2* mRNA promotes cell cycling within the ectoderm and inhibits endogenous neurogenesis (Richard-Parpaillon et al., 2004). *Cyclin A*/*cdk2* overexpression also inhibited neurogenesis in the presence of ectopic *xNgn2* mRNA, indicating that inhibition occurs at the level of post-translational modification of xNgn2 or, potentially, of a downstream target (Fig. 6A,B). 9S-A xNgn2 induced substantially greater ectopic neurogenesis in both the neural plate and epidermis than the wild-type protein, as expected. Strikingly, this extensive ectopic neurogenesis induced by *9S-A xNgn2* overexpression was unaffected by *cyclin A*/*cdk2* overexpression (Fig. 6A,B). This demonstrates that enhanced cyclin/cdk kinase activity, which promotes more rapid cell cycling (Richard-Parpaillon et al., 2004), also directly inhibits the neurogenesis-inducing ability of xNgn2 protein in vivo by post-translational modification.

Cdk inhibitors (cdkis) accumulate as the cell cycle lengthens and their expression is associated with both a drop in cdk kinase levels and neuronal differentiation (e.g. Cremisi et al., 2003; Vernon et al., 2003; Nguyen et al., 2006). We have previously shown that cdkis have an additional role in neurogenesis independent of, but complementary to, their role in inhibiting cyclin/cdk kinase activity: the *Xenopus* Cip/Kip family cdk inhibitor, Xic1, is required for neuronal differentiation in the developing embryo, where it functions to stabilise xNgn2 protein independently of its ability to inhibit overall cdk kinase activity. Similarly, $p27^{Kip1}$ stabilises Ngn2 in the mouse cortex (Nguyen et al., 2006).

Because of their more stable association with promoter DNA, we hypothesised that 9S-A xNgn2-E protein complexes might be less dependent on the presence of Xic1 to enhance Ngn2 protein stability and hence drive neuronal differentiation in vivo than the wild-type protein. To test this, we investigated the ability of *xNgn2* and *9S-A xNgn2* to induce neurogenesis in the presence of a Xic1 morpholino (Xic1 Mo), which has previously been shown to abolish Xic1 protein expression and inhibit Ngn2-dependent neuronal differentiation (Vernon et al., 2003). As expected, Xic1 Mo injection significantly reduced endogenous neurogenesis, as assayed by in situ hybridisation, whereas the control morpholino (Con Mo) had little effect (Fig. 7A,B) (Vernon et al., 2003). The low doses of *xNgn2* mRNA chosen to achieve near-physiological levels of expression induced modest but clear ectopic neurogenesis both within and outside the neural plate in the presence of Con Mo. Both the ectopic and endogenous neurogenesis seen in *xNgn2*-injected embryos were largely abolished by co-injection of Xic1 Mo, confirming that wild-type xNgn2 requires Xic1 for full activity (Fig. 7A,B) (Vernon et al., 2003).

As expected, extensive neurogenesis was induced by *9S-A xNgn2* mRNA plus Con Mo both within and outside the neural plate. However, in contrast to *xNgn2*, *9S-A xNgn2* could induce

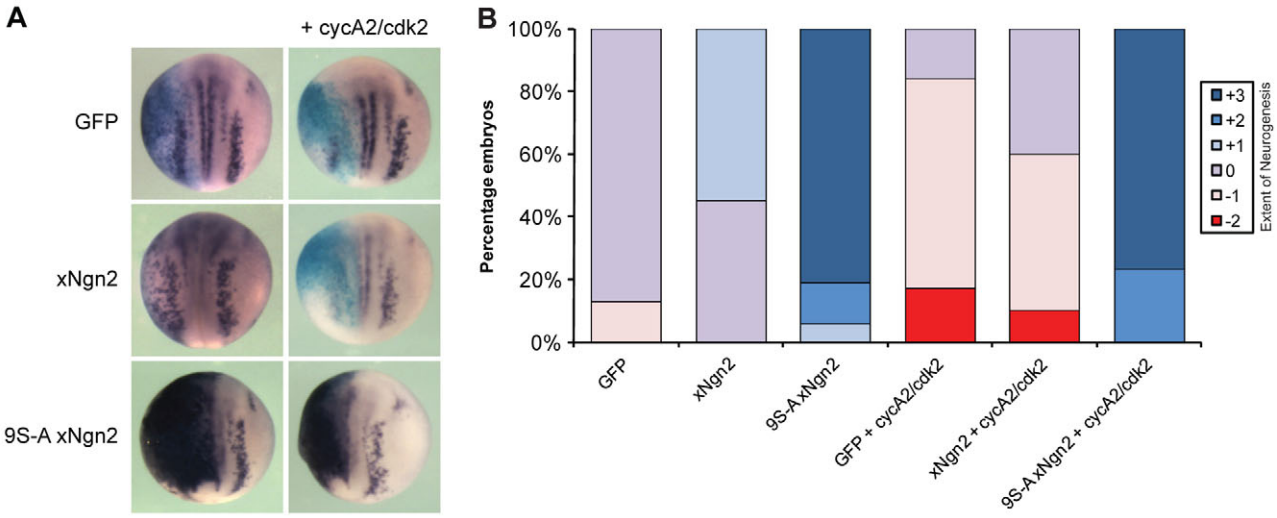

Fig. 6. 9S-A xNgn2 is resistant to cyclin A2/cdk2-mediated suppression of neurogenesis in vivo. (**A**) *Xenopus* embryos were injected (left side) in one of two cells with 20 pg *xNgn2* or *9S-A xNgn2* mRNA, together with 500 pg *cyclin A2* and *cdk2* mRNA, assaying for expression of neural *β-tubulin* at stage 15 by in situ hybridisation. (**B**) Semi-quantitative analysis of in situ hybridisation data. The number of embryos scored was 48-86 per condition. Neurogenesis was enhanced (+3, +2, +1), the same as (0) or reduced (–1, –2, –3) compared with the uninjected side (see Fig. S8 in the supplementary material).

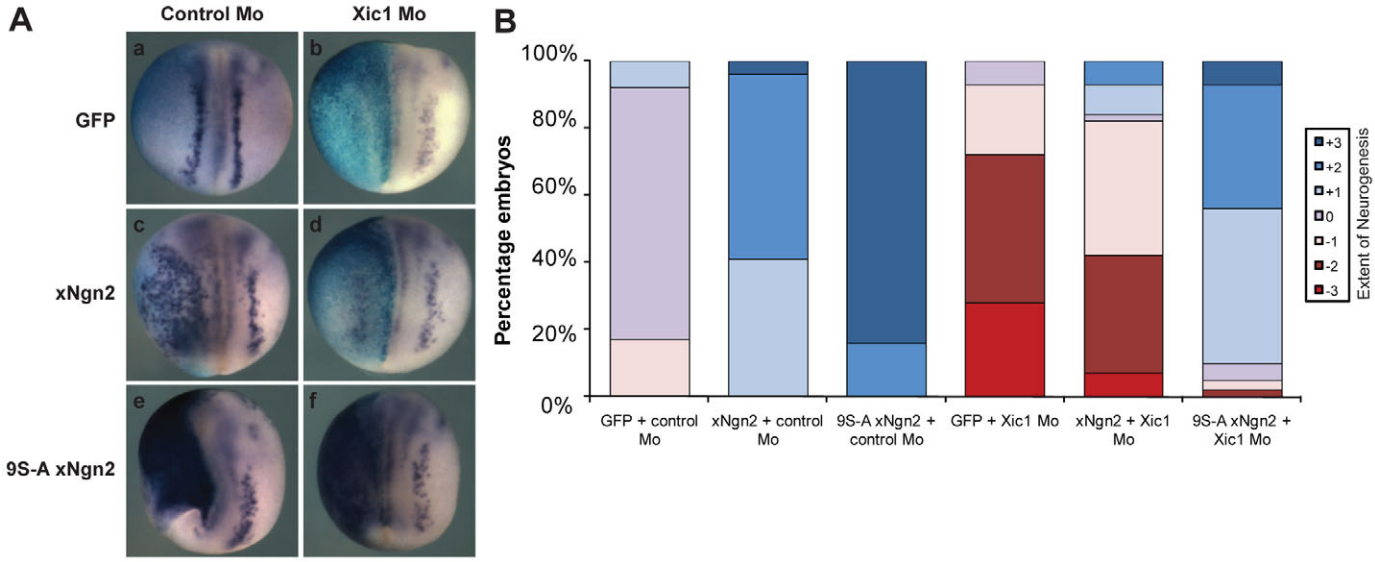

Fig. 7. 9S-A xNgn2 does not require the cdk inhibitor Xic1 for activity. (**A**) *Xenopus* embryos were injected (left side) in one of four cells (dorsally targeted) with 20 pg mRNA as indicated, together with 20 ng of either control (**a**,**c**,**e**) or Xic1 (**b**,**d**,**f**) morpholino, fixed at stage 15 and subject to in situ hybridisation for *neural* β-*tubulin* expression. (**B**) Semi-quantitative analysis of in situ hybridisation data. The number of embryos scored was 43-59 per condition. Neurogenesis was enhanced (+3, +2, +1), the same as (0) or reduced (–1, –2, –3) compared with the uninjected side (see Fig. S8 in the supplementary material for examples of the scoring method).

substantial neurogenesis even in the presence of Xic1 Mo (Fig. 7A,B). Thus, 9S-A xNgn2 has a reduced requirement for Xic1 compared with the wild-type protein, consistent with the enhanced stability of un(der)phosphorylated Ngn2.

DISCUSSION

Ngn2 acts as a master regulatory transcription factor that controls the balance between progenitor maintenance and differentiation in response to increasing cell cycle length as development progresses. We show that this is achieved by multi-site phosphorylation of Ngn2, which is quantitatively sensitive to cdk levels and quantitatively regulates the stability of Ngn2 binding to promoters of key downstream transcriptional targets, resulting in the regulation of neuronal differentiation.

Transcription factors undergo dynamic binding cycles on promoters. Increased dwell time on promoters is associated with more active transcription; for example, a slower exchange rate of the glucocorticoid receptor at promoters would promote the assembly of additional components required for chromatin remodelling and transcriptional activation (Stavreva et al., 2004; Hager et al., 2009). The requirement for stable association of Ngn2 with the target promoter to drive differentiation leads directly to a mechanism whereby post-translational modification of Ngn2 in response to the cellular environment, and the cdk kinase level in particular, can influence the propensity to differentiate.

Cdk-dependent inhibitory phosphorylation of Ngn2 complements another level of cell cycle-dependent post-translational regulation of Ngn2. We have previously shown that the cdkis $p27^{Xic1}$ in *Xenopus* and $p27^{Kip1}$ (Cdkn1b) in mouse are required for transcriptional activity of Ngn2 (Nguyen et al., 2006; Vernon et al., 2003). Acting independently of (but complementary to) their ability to inhibit cyclins and cdks, these cdkis inhibit ubiquitin-mediated proteolysis of Ngn2 protein, thus facilitating neuronal differentiation. In addition to this stabilising effect, accumulation of cdkis in neural precursors with lengthening cell cycles will also directly inhibit cdk activity, reducing the inhibitory phosphorylation of Ngn2 and so enhancing its transcriptional activity on differentiation targets. However, it should be noted that these cdkis themselves have not been shown to be direct transcriptional targets of Ngn2 (Seo et al., 2007).

From our biochemical in vitro assays, coupled with overexpression experiments in both cultured P19 cells and *Xenopus* embryos, we propose the following model (Fig. 8). In cycling cells, cdk levels rise rapidly on transition through late G1 and S phase into G2 and mitosis, promoting increasing phosphorylation of Ngn2 by cdk2 and cdk1, and resulting in reduced promoter occupancy, which is insufficient to activate the Ngn2-responsive promoters of genes required for neuronal differentiation, such as *NeuroD*. By contrast, cell cycle lengthening results in a longer time spent in G1, where cdk levels are low and cdk inhibitors accumulate. This favours un(der)phosphorylated, more stable Ngn2, which binds E box DNA more tightly. This greater promoter occupancy would be permissive for transcription of Ngn2 targets driving neuronal differentiation. Moreover, the graded response of neural β-tubulin to Ngn2 phosphorylation on additive sites allows cdk levels to be interpreted in a rheostat-like manner (Deshaies and Ferrell, 2001; Pufall et al., 2005). Here, we have concentrated on cdk-dependent phosphorylation of Ngn2. However, multi-site phosphorylation could be used as a mechanism to integrate a range of signals that culminate in proline-directed kinase activity.

The promoter of the *NeuroD* gene is known to respond slowly to Ngn2 expression and to require extensive chromatin modification for activation (Koyano-Nakagawa et al., 1999), which fits with our model in which stable promoter association is required to drive neuronal differentiation. Ngn2 has many direct downstream targets with potentially differing requirements for epigenetic modification, and hence for recruitment of chromatin modifiers, before activation (Koyano-Nakagawa et al., 1999; Seo et al., 2007). Different promoters might therefore respond

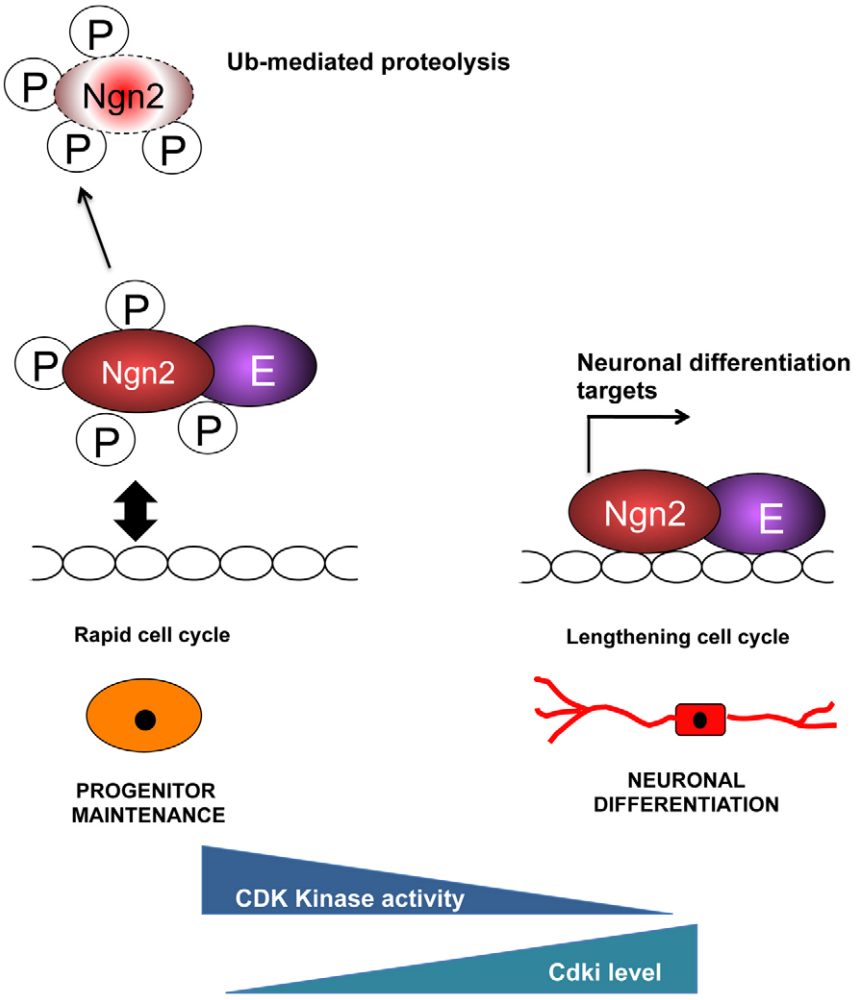

Fig. 8. Model of control of neuronal differentiation via cell cycle length and Ngn2 phosphorylation. Phosphorylation of Ngn2 protein occurs in rapid progenitor cell cycles. Cell cycle lengthening results in an accumulation of un(der)phosphorylated Ngn2, enhancing promoter binding and resulting in the activation of downstream target genes that drive differentiation. E, E protein; Ub, ubiquitin; P, phosphorylation.

differently to changes in Ngn2 phosphorylation status, affecting the frequency/duration of promoter occupancy, and we are currently exploring this possibility.

Our analyses indicate the importance of the number of SP sites modified, rather than their precise location, for regulation of protein function (Fig. 5). Native Ngn2 might be largely unstructured, like the related protein Ngn1 (Aguado-Llera et al., 2010), and hence might have limited structural constraints for phosphorylation on SP sites. Several classes of transcription factors have been identified in which unstructured N- and C-terminal extensions from the known DNA-binding domains contribute to DNA-binding affinity (Crane-Robinson et al., 2006), which would in turn affect the frequency and duration of DNA-protein binding cycles (Michel, 2009). Our data demonstrate that phosphorylation of residues in both the N- and C-termini quantitatively reduce Ngn2 DNA-binding activity.

In summary, we have shown here that Ngn2 is directly phosphorylated at multiple sites by cdk kinases and that this directly controls its ability to drive neuronal differentiation. Hence, we have uncovered a molecular mechanism whereby cell cycle lengthening can directly trigger neuronal differentiation.

Acknowledgements
We thank Helen Wise, Christelle Fiore-Heriche, Romana Kucerova and Jon Vosper for important initial observations leading up to this study; Ian Horan, Kate Wilson, Chris Hurley and Venkat Pisupati for technical assistance; and Jeremy Gunewardena, Hanno Steen and Bill Harris for helpful discussions.

Funding
This work was supported by MRC Research Grant G0700758, an MRC DTA studentship (G.M.) and a Cancer Research UK Studentship (C.H.). F.G. is supported by a Grant-in-Aid from the Medical Research Council (U117570528). M.K. and R.D. acknowledge a grant from the National Institute of General Medical Sciences (GM26875). Deposited in PMC for release after 6 months.

Competing interests statement
The authors declare no competing financial interests.

Supplementary material
Supplementary material for this article is available at
http://dev.biologists.org/lookup/suppl/doi:10.1242/dev.067900/-/DC1

References

Aguado-Llera, D., Goormaghtigh, E., de Geest, N., Quan, X. J., Prieto, A., Hassan, B. A., Gomez, J. and Neira, J. L. (2010). The basic helix-loop-helix region of human neurogenin 1 is a monomeric natively unfolded protein which forms a "fuzzy" complex upon DNA binding. *Biochemistry* **49**, 1577-1589.
Bain, J., Plater, L., Elliott, M., Shpiro, N., Hastie, C. J., McLauchlan, H., Klevernic, I., Arthur, J. S., Alessi, D. R. and Cohen, P. (2007). The selectivity of protein kinase inhibitors: a further update. *Biochem. J.* **408**, 297-315.
Bertrand, N., Castro, D. S. and Guillemot, F. (2002). Proneural genes and the specification of neural cell types. *Nat. Rev. Neurosci.* **3**, 517-530.
Crane-Robinson, C., Dragan, A. I. and Privalov, P. L. (2006). The extended arms of DNA-binding domains: a tale of tails. *Trends Biochem. Sci.* **31**, 547-552.
Cremisi, F., Philpott, A. and Ohnuma, S. (2003). Cell cycle and cell fate interactions in neural development. *Curr. Opin. Neurobiol.* **13**, 26-33.
Deibler, R. W. and Kirschner, M. W. (2010). Quantitative reconstitution of mitotic CDK1 activation in somatic cell extracts. *Mol. Cell* **37**, 753-767.

Deshaies, R. J. and Ferrell, J. E., Jr (2001). Multisite phosphorylation and the countdown to S phase. *Cell* **107**, 819-822.
Errico, A., Deshmukh, K., Tanaka, Y., Pozniakovsky, A. and Hunt, T. (2010). Identification of substrates for cyclin dependent kinases. *Adv. Enzyme Regul.* **50**, 375-399.
Farah, M. H., Olson, J. M., Sucic, H. B., Hume, R. I., Tapscott, S. J. and Turner, D. L. (2000). Generation of neurons by transient expression of neural bHLH proteins in mammalian cells. *Development* **127**, 693-702.
Hager, G. L., McNally, J. G. and Misteli, T. (2009). Transcription dynamics. *Mol. Cell* **35**, 741-753.
Hand, R., Bortone, D., Mattar, P., Nguyen, L., Heng, J. I., Guerrier, S., Boutt, E., Peters, E., Barnes, A. P., Parras, C. et al. (2005). Phosphorylation of Neurogenin2 specifies the migration properties and the dendritic morphology of pyramidal neurons in the neocortex. *Neuron* **48**, 45-62.
King, R. W., Glotzer, M. and Kirschner, M. W. (1996). Mutagenic analysis of the destruction signal of mitotic cyclins and structural characterization of ubiquitinated intermediates. *Mol. Biol. Cell* **7**, 1343-1357.
Koyano-Nakagawa, N., Wettstein, D. and Kintner, C. (1999). Activation of Xenopus genes required for lateral inhibition and neuronal differentiation during primary neurogenesis. *Mol. Cell. Neurosci.* **14**, 327-339.
Lange, C. and Calegari, F. (2010). Cdks and cyclins link G(1) length and differentiation of embryonic, neural and hematopoietic stem cells. *Cell Cycle* **9**, 1893-1900.
Lange, C., Huttner, W. B. and Calegari, F. (2009). Cdk4/cyclinD1 overexpression in neural stem cells shortens G1, delays neurogenesis, and promotes the generation and expansion of basal progenitors. *Cell Stem Cell* **5**, 320-331.
Ma, Q., Kintner, C. and Anderson, D. J. (1996). Identification of neurogenin, a vertebrate neuronal determination gene. *Cell* **87**, 43-52.
Ma, Y. C., Song, M. R., Park, J. P., Ho, H.-Y. H., Hu, L., Kurtev, M. V., Zieg, J., Ma, Q., Pfaff, S. L. and Greenberg, M. E. (2008). Regulation of motor neuron specification by phosphorylation of neurogenin 2. *Neuron* **58**, 65-77.
Michel, D. (2009). Fine tuning gene expression through short DNA-protein binding cycles. *Biochimie* **91**, 933-941.
Miyata, T., Kawaguchi, D., Kawaguchi, A. and Gotoh, Y. (2010). Mechanisms that regulate the number of neurons during mouse neocortical development. *Curr. Opin. Neurobiol.* **20**, 22-28.
Nguyen, L., Besson, A., Heng, J. I., Schuurmans, C., Teboul, L., Parras, C., Philpott, A., Roberts, J. M. and Guillemot, F. (2006). p27kip1 independently promotes neuronal differentiation and migration in the cerebral cortex. *Genes Dev.* **20**, 1511-1524.
Nieber, F., Pieler, T. and Henningfeld, K. A. (2009). Comparative expression analysis of the neurogenins in Xenopus tropicalis and Xenopus laevis. *Dev. Dyn.* **238**, 451-458.
Pufall, M. A., Lee, G. M., Nelson, M. L., Kang, H. S., Velyvis, A., Kay, L. E., McIntosh, L. P. and Graves, B. J. (2005). Variable control of Ets-1 DNA binding by multiple phosphates in an unstructured region. *Science* **309**, 142-145.
Richard-Parpaillon, L., Cosgrove, R. A., Devine, C., Vernon, A. E. and Philpott, A. (2004). G1/S phase cyclin-dependent kinase overexpression perturbs early development and delays tissue-specific differentiation in Xenopus *Development* **131**, 2577-2586.
Seo, S., Lim, J. W., Yellajoshyula, D., Chang, L. W. and Kroll, K. L. (2007). Neurogenin and NeuroD direct transcriptional targets and their regulatory enhancers. *EMBO J.* **26**, 5093-5108.
Shimojo, H., Ohtsuka, T. and Kageyama, R. (2008). Oscillations in notch signaling regulate maintenance of neural progenitors. *Neuron* **58**, 52-64.
Stavreva, D. A., Muller, W. G., Hager, G. L., Smith, C. L. and McNally, J. G. (2004). Rapid glucocorticoid receptor exchange at a promoter is coupled to transcription and regulated by chaperones and proteasomes. *Mol. Cell. Biol.* **24**, 2682-2697.
Ubersax, J. A. and Ferrell, J. E., Jr (2007). Mechanisms of specificity in protein phosphorylation. *Nat. Rev. Mol. Cell Biol.* **8**, 530-541.
Vernon, A. E., Devine, C. and Philpott, A. (2003). The cdk inhibitor p27Xic1 is required for differentiation of primary neurones in Xenopus. *Development* **130**, 85-92.
Vosper, J. M., Fiore-Heriche, C. S., Horan, I., Wilson, K., Wise, H. and Philpott, A. (2007). Regulation of neurogenin stability by ubiquitin-mediated proteolysis. *Biochem. J.* **407**, 277-284.
Vosper, J. M., McDowell, G. S., Hindley, C. J., Fiore-Heriche, C. S., Kucerova, R., Horan, I. and Philpott, A. (2009). Ubiquitylation on canonical and non-canonical sites targets the transcription factor neurogenin for ubiquitin-mediated proteolysis. *J. Biol. Chem.* **284**, 15458-15468.

A

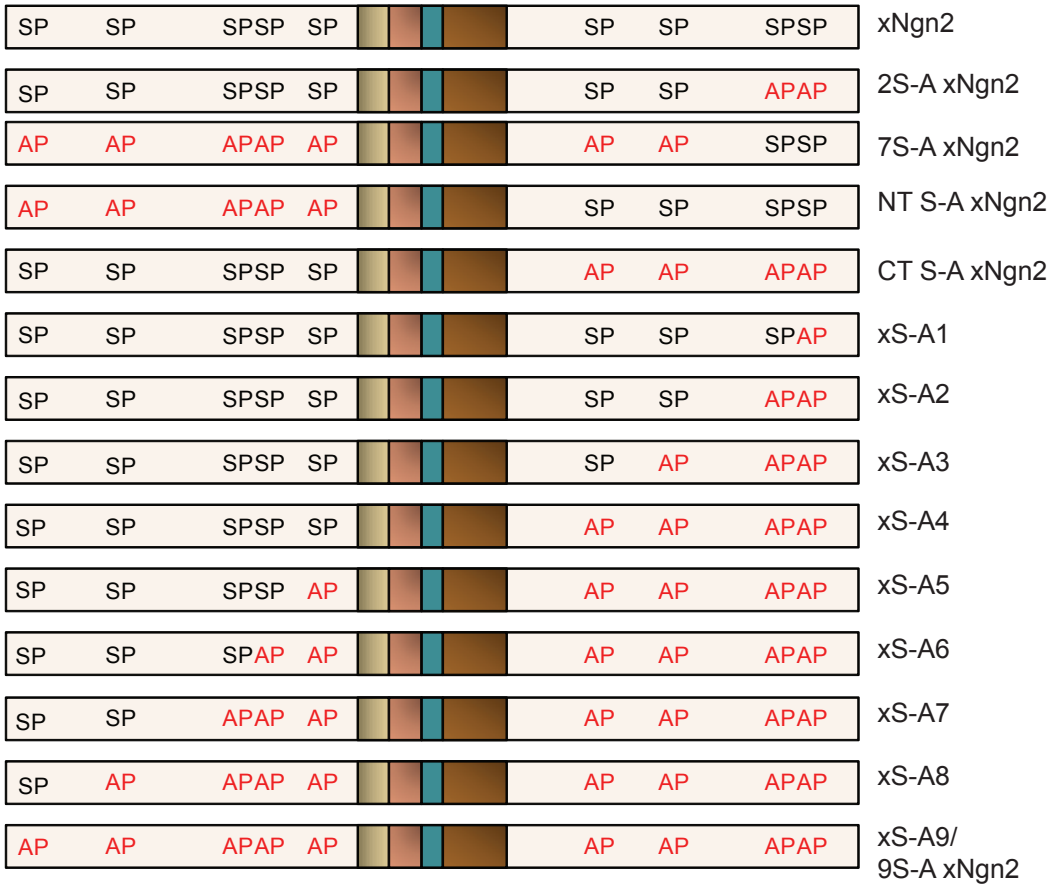
SP SP SPSP SP SP SP SPSP
xNgn2
SP SP SPSP SP SP SP APAP
2S-A xNgn2
AP AP APAP AP AP AP SPSP
7S-A xNgn2
AP AP APAP AP SP SP SPSP
NT S-A xNgn2
SP SP SPSP SP AP AP APAP
CT S-A xNgn2
SP SP SPSP SP SP SP SPAP
xS-A1
SP SP SPSP SP SP SP APAP
xS-A2
SP SP SPSP SP SP AP APAP
xS-A3
SP SP SPSP SP AP AP APAP
xS-A4
SP SP SPSP AP AP AP APAP
xS-A5
SP SP SPAP AP AP AP APAP
xS-A6
SP SP APAP AP AP AP APAP
xS-A7
SP AP APAP AP AP AP APAP
xS-A8
AP AP APAP AP AP AP APAP
xS-A9/
9S-A xNgn2

B

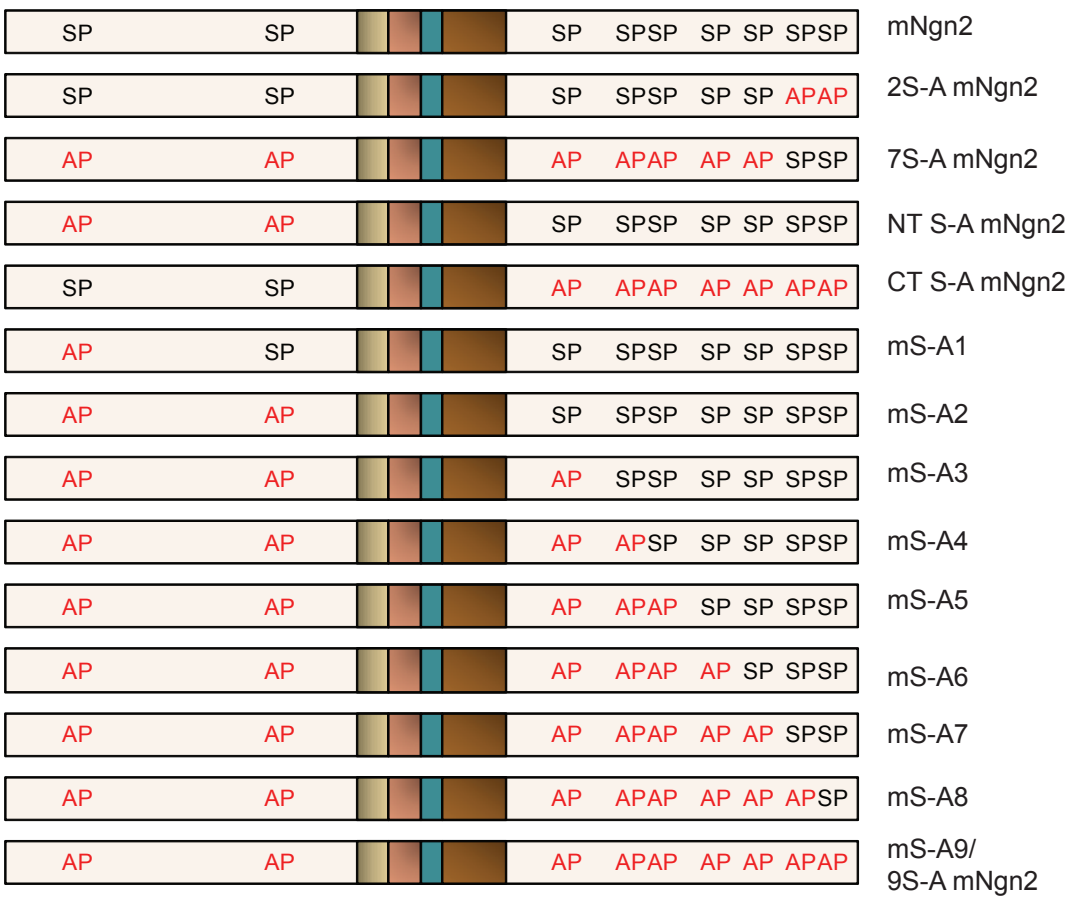
SP SP SP SPSP SP SP SPSP
mNgn2
SP SP SP SPSP SP SP APAP
2S-A mNgn2
AP AP AP APAP AP AP SPSP
7S-A mNgn2
AP AP SP SPSP SP SP SPSP
NT S-A mNgn2
SP SP AP APAP AP AP APAP
CT S-A mNgn2
AP SP SP SPSP SP SP SPSP
mS-A1
AP AP SP SPSP SP SP SPSP
mS-A2
AP AP AP SPSP SP SP SPSP
mS-A3
AP AP AP APSP SP SP SPSP
mS-A4
AP AP AP APAP SP SP SPSP
mS-A5
AP AP AP APAP AP SP SPSP
mS-A6
AP AP AP APAP AP AP SPSP
mS-A7
AP AP AP APAP AP AP APSP
mS-A8
AP AP AP APAP AP AP APAP
mS-A9/
9S-A mNgn2

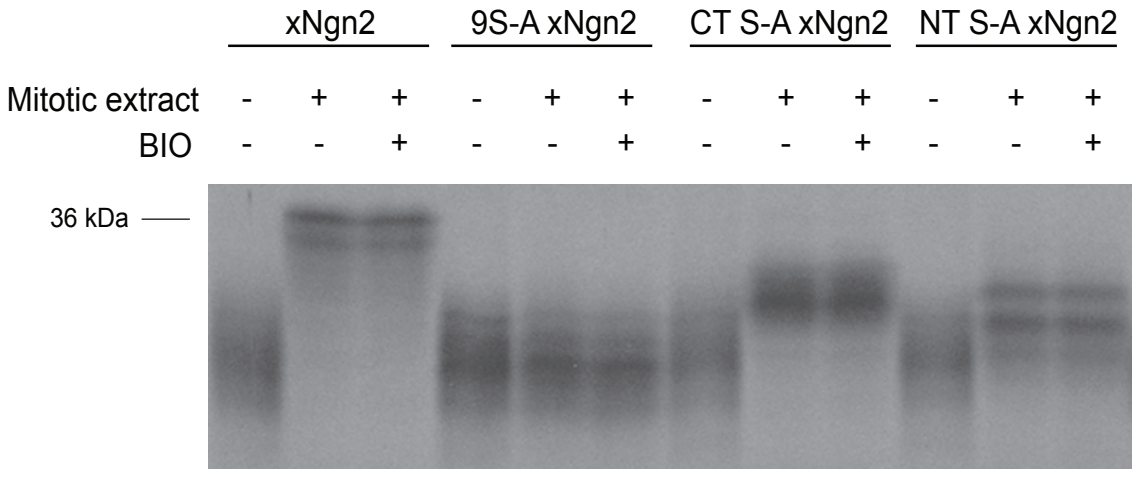
xNgn2
9S-A xNgn2
CT S-A xNgn2
NT S-A xNgn2
Mitotic extract - + + - + + - + + - + +
BIO - - + - - + - - + - - +
36 kDa

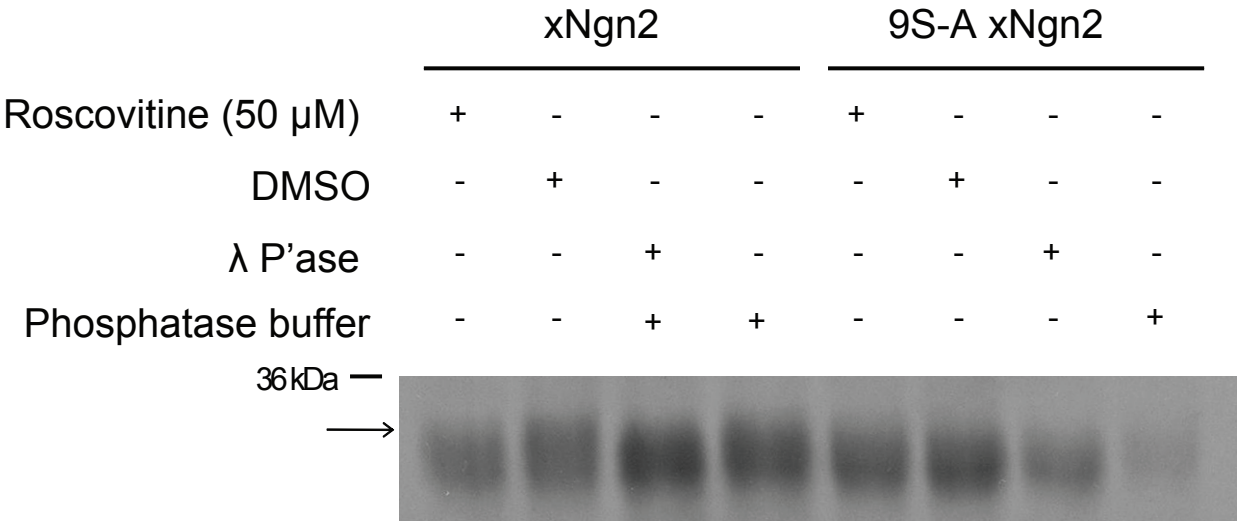
xNgn2
9S-A xNgn2
Roscovitine (50 μM) + - - - + - - -
DMSO - + - - - + - -
λ P'ase - - + - - - + -
Phosphatase buffer - - + + - - - +
36 kDa

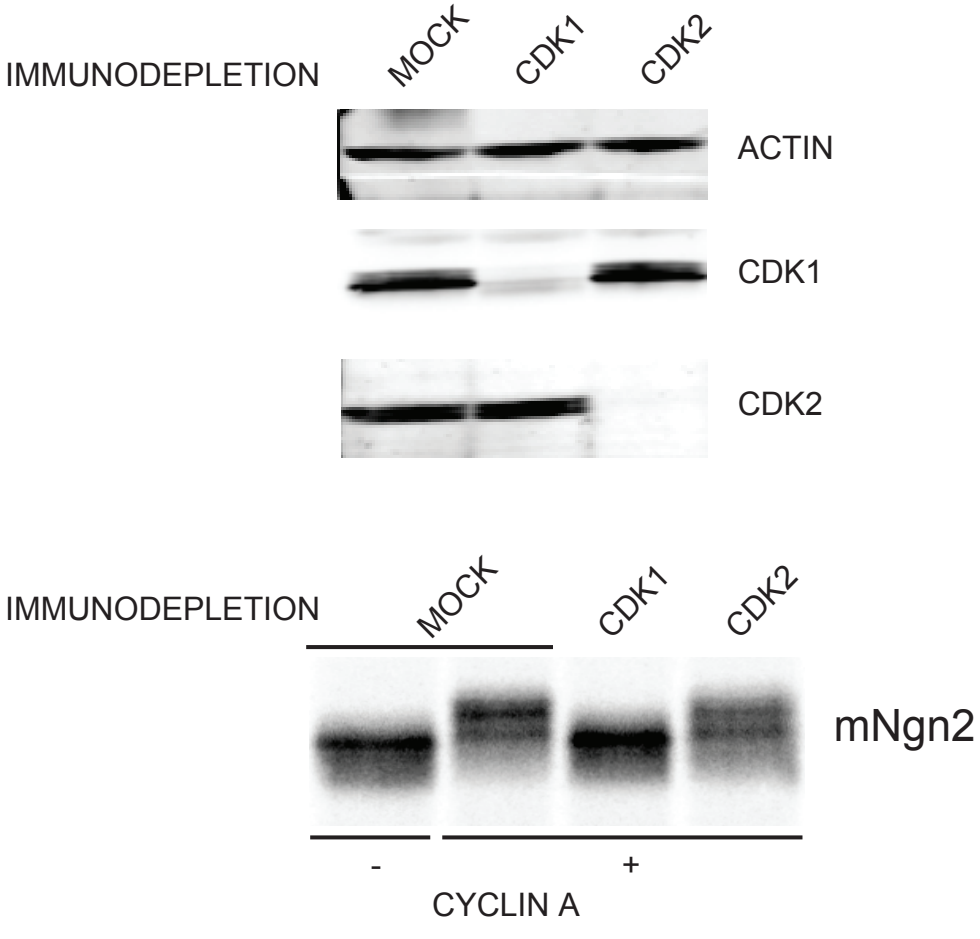
IMMUNODEPLETION
MOCK
CDK1
CDK2
ACTIN
CDK1
CDK2
IMMUNODEPLETION
MOCK
CDK1
CDK2
mNgn2
-
+
CYCLIN A

A

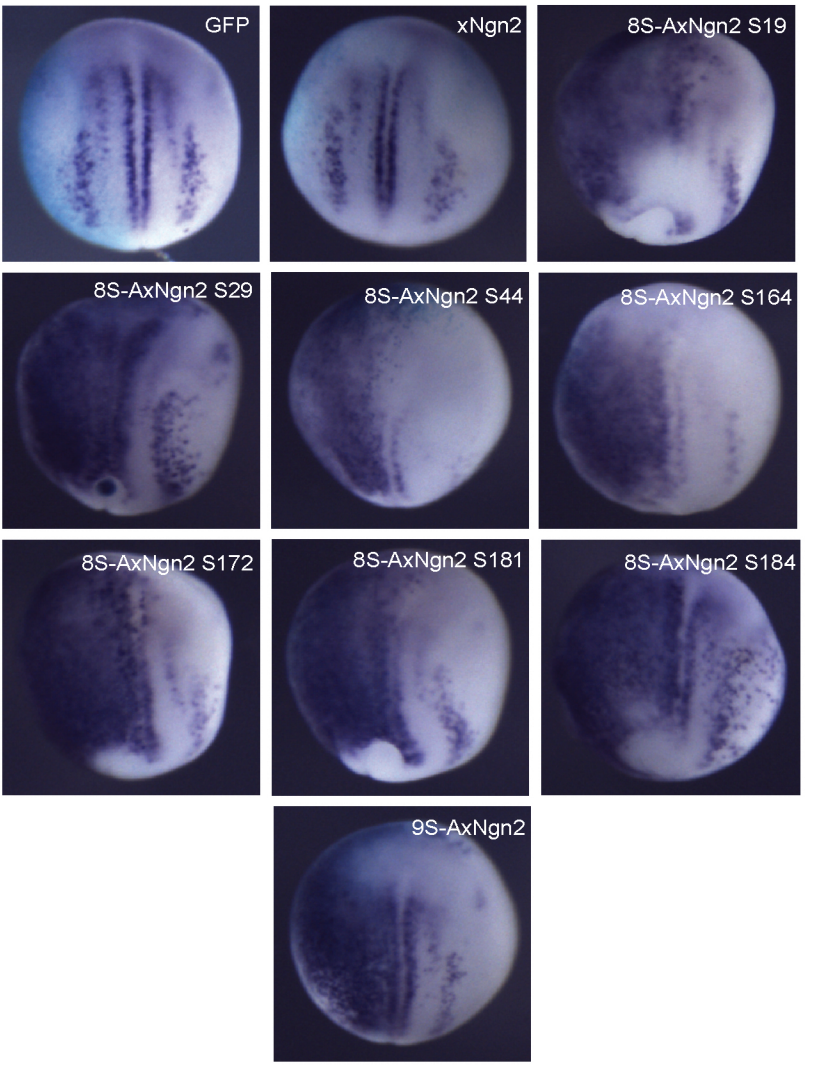
GFP
xNgn2
8S-AxNgn2 S19
8S-AxNgn2 S29
8S-AxNgn2 S44
8S-AxNgn2 S164
8S-AxNgn2 S172
8S-AxNgn2 S181
8S-AxNgn2 S184
9S-AxNgn2

B

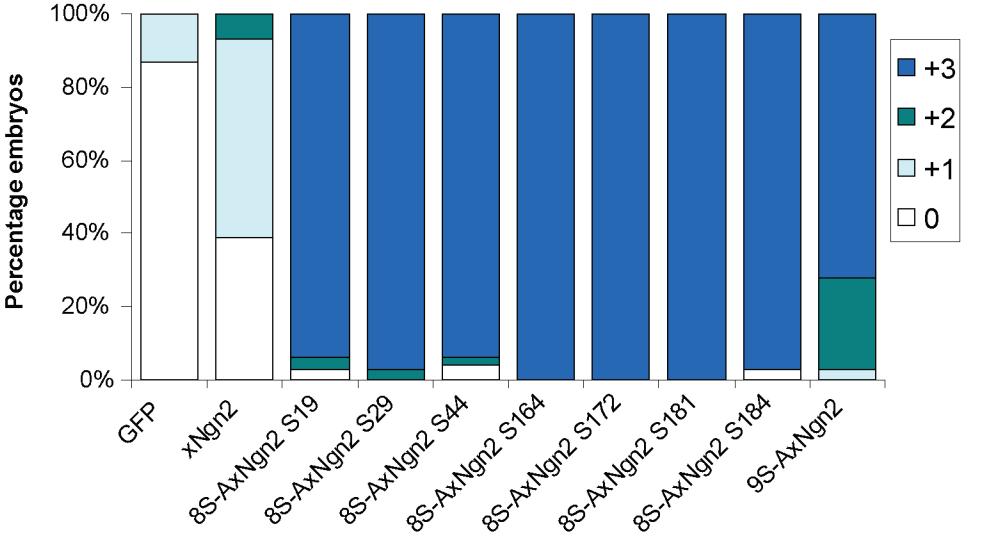
Percentage embryos
100%
80%
60%
40%
20%
0%
+3
+2
+1
0
GFP
xNgn2
8S-AxNgn2 S19
8S-AxNgn2 S29
8S-AxNgn2 S44
8S-AxNgn2 S164
8S-AxNgn2 S172
8S-AxNgn2 S181
8S-AxNgn2 S184
9S-AxNgn2

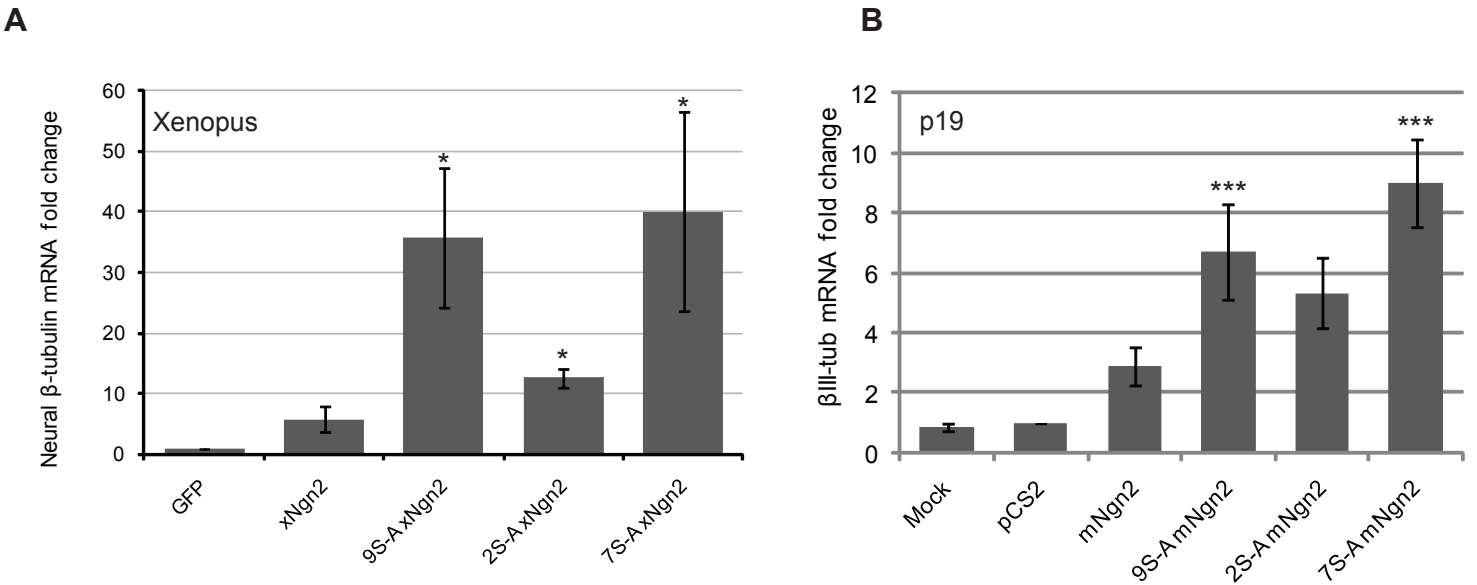
A
Xenopus
Neural β-tubulin mRNA fold change
60
50
40
30
20
10
0
*
*
*
GFP
xNgn2
9S-AxNgn2
2S-AxNgn2
7S-AxNgn2
B
p19
βIII-tub mRNA fold change
12
10
8
6
4
2
0
***
***
Mock
pCS2
mNgn2
9S-AmNgn2
2S-AmNgn2
7S-AmNgn2

A

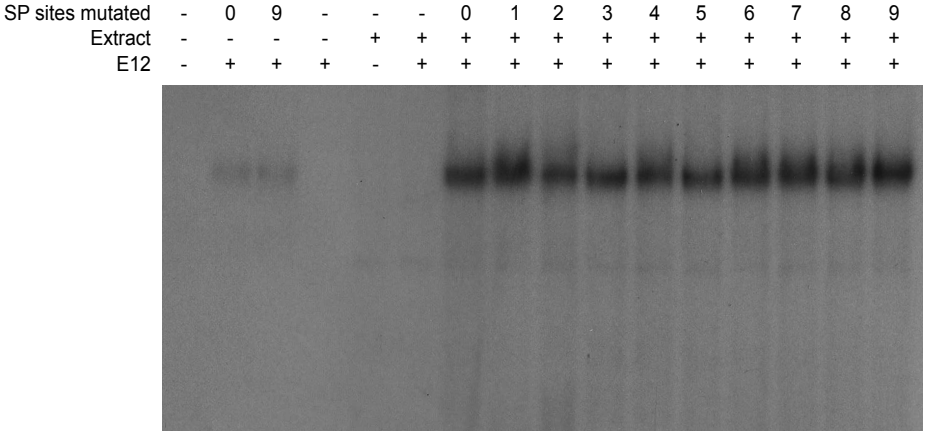
SP sites mutated - 0 9 - - - 0 1 2 3 4 5 6 7 8 9
Extract - - - - + + + + + + + + + + + +
E12 - + + + - + + + + + + + + + + +

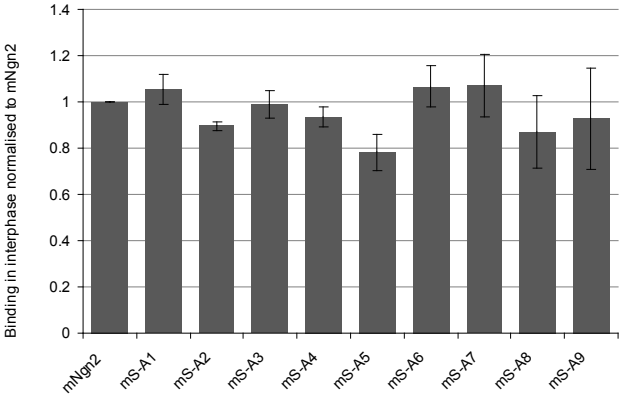
Binding in interphase normalised to mNgn2
1.4
1.2
1
0.8
0.6
0.4
0.2
0
mNgn2
mS-A1
mS-A2
mS-A3
mS-A4
mS-A5
mS-A6
mS-A7
mS-A8
mS-A9

B

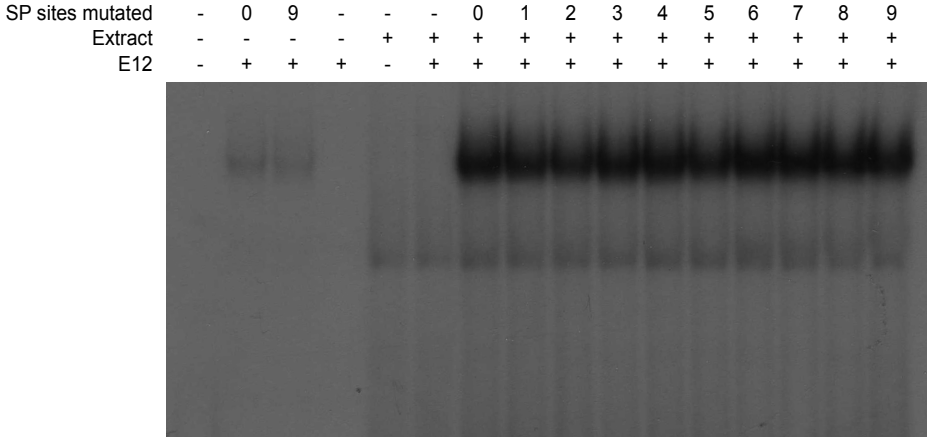
SP sites mutated - 0 9 - - - 0 1 2 3 4 5 6 7 8 9
Extract - - - - + + + + + + + + + + + +
E12 - + + + - + + + + + + + + + + +

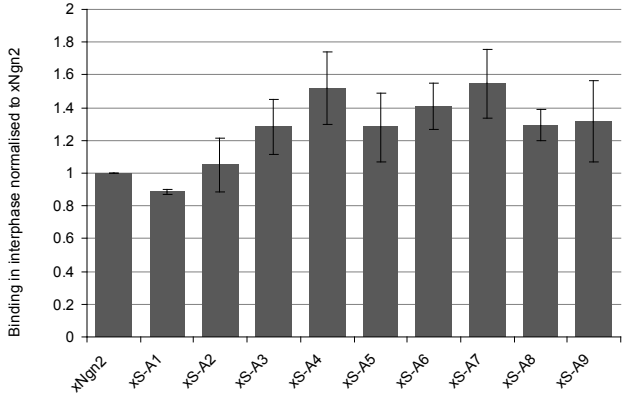
Binding in interphase normalised to xNgn2
2
1.8
1.6
1.4
1.2
1
0.8
0.6
0.4
0.2
0
xNgn2
xS-A1
xS-A2
xS-A3
xS-A4
xS-A5
xS-A6
xS-A7
xS-A8
xS-A9

Increase in neurogenesis

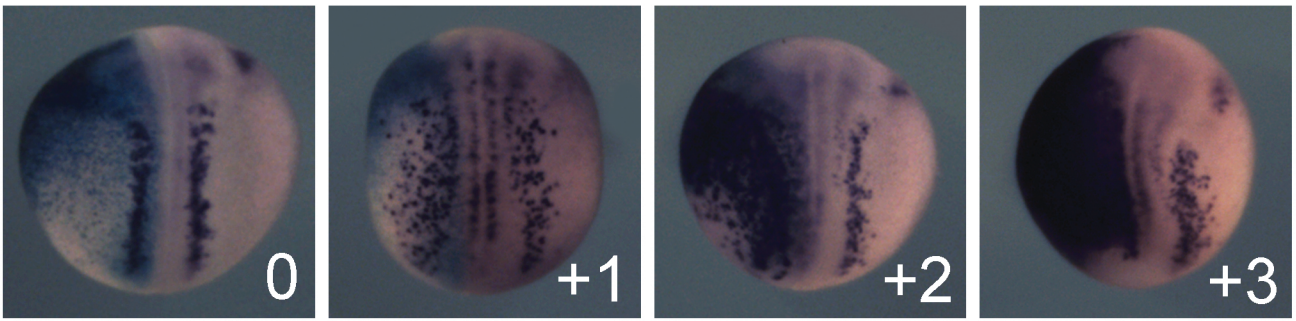

Decrease in neurogenesis

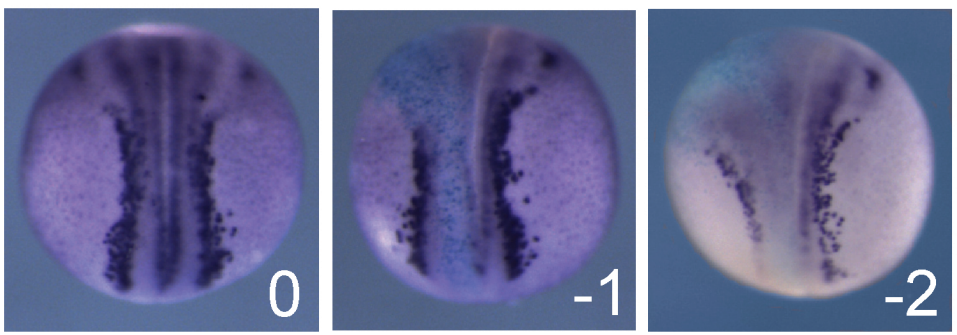

Table S1. Primers for quantitative real-time PCR

Primer	Sequence (5′ to 3′)
m_βIII-tubulin Fwd	TCCGCCTGCCTTTTCGTCT
m_βIII-tubulin rev	CCAGTTGTTGCCAGCACCAC
xNeural-β-tub_Fwd	ACACGGCATTGATCCTACAG
xNeural-β-tub_rev	AGCTCCTTCGGTGTAATGAC
mBactin Fwd	CAGGGTGTGATGGTGGGAATG
mBactin rev	ATGGCTGGGGTGTTGAAGGTC
mGAPDH Fwd	GAAGGTCGGTGTGAACGGATTT
mGAPDH rev	CATTTGATGTTAGTGGGGTCTCGC
xODC_Fwd	GAATCACCCGAATGCAAAGC
xODC_rev	CCACTGCCAACATGGAAACTC